Journal of
Water & Climate Change

IWA PUBLISHING

Journal of Water and Climate Change Vol 14 No 1, 330 doi: 10.2166/wcc.2022.475

Preliminary assessment of near-shorewave energy potential in the Mozambique Channel

Alberto Filimão Sitoe[a,b], A. M. Hoguane[c] and Soufiane Haddout[d,*]

[a] Faculty of Natural and Exact Science, Save University (UniSave), Chongoene, Mozambique
[b] Department of Physics, Faculty of Science, Eduardo Mondlane University (UEM), Maputo, Mozambique
[c] Centre for Marine Research and Technology (CePTMar), Eduardo Mondlane University, P.O. Box 128, Quelimane, Mozambique
[d] Department of Physics, Faculty of Science, Ibn Tofail University, B.P. 133, Kenitra, Morocco
*Corresponding author. E-mail: soufian.haddout@gmail.com

ABSTRACT

This paper presents the results of a study of ocean wave energy in the Mozambique Channel, an open channel located in the Western Indian Ocean and oriented north-southwards. Weekly data of significant wave height and wave period, obtained from marine-analyst, on the web, were analysed in 10 selected coastal sites, 5 on each side of the channel. The channel receives swell waves from the extratropical South Indian Ocean in the south and monsoon-generated swell from the north, modified by trade winds and cyclones. The results indicate that the waves are highly variable (≥80%), with high (1.5–2 m on average), longer (8–20 s, on average), and more energetic (10–23 kW m^{-1}, on average) waves found in the southern part of the channel, followed by the northern part of the channel (1.2–1.4 m, 6–8 s, 6–7 kW m^{-1}, on average), with the middle part displaying a lower energy (6 kW m^{-1}, on average) wave climate. Peaks of high waves (up to 5 m) and high-energy waves (up to 90 kW m^{-1}), attributed to storm conditions, were observed throughout the study period. Despite high variability in wave characteristics, the probability of waves exceeding the threshold values for viable exploitation for electricity production was about 61 and 63% for the western and eastern sides of the channel, respectively.

Key words: desalination, irrigation, open channel, swell, wave energy applications, wave variability

HIGHLIGHTS

- Ocean wave energy in the Mozambique Channel, an open channel located in the Western Indian Ocean and oriented north-southwards is studied.
- A recommended location for the deployment of energy extraction devices for electricity production.

GRAPHICAL ABSTRACT

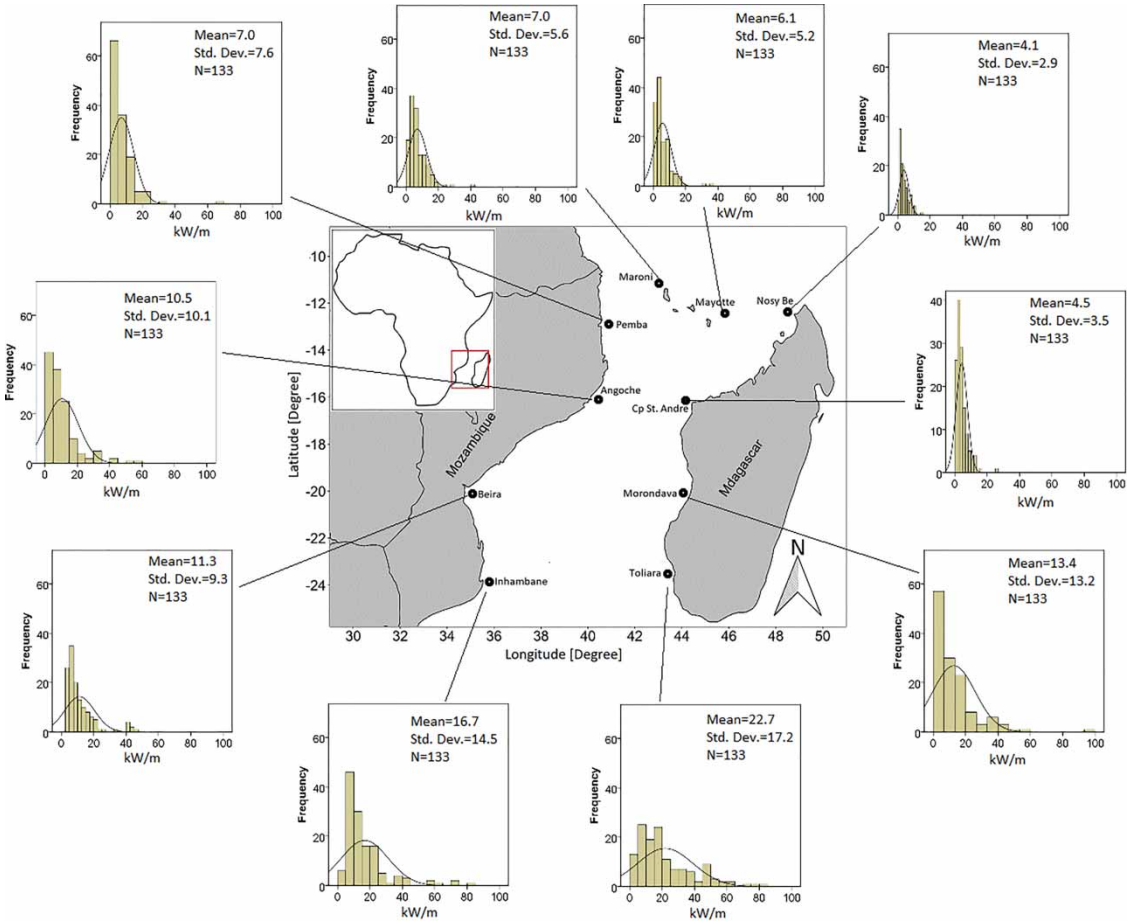

1. INTRODUCTION

In view of the foreseen increase in energy demand (Hafner *et al.* 2018; Warner & Jones 2018) and the challenges imposed by climate change, which require the reduction in the use of fossil fuels, the fostering of sources of renewable energy (Deichmann *et al.* 2011; Ouedraogo 2017; Warner & Jones 2018; United Nations Department of Economic and Social Affairs, Sustainable Development Goals 2021) is becoming a priority for the world. Ocean wave energy, which is being exploited on a trial basis in South Africa (ESI Africa South Africa: wave energy power plant development 2015), has the potential to be a viable alternative source of clean energy to remote coastal households, thus reducing the energy-deficit (Owusu & Asumadu-Sarkodie 2016; Hafner *et al.* 2018) in Sub-Saharan Africa. Regions of high wave energy in Sub-Saharan Africa have been identified on the coast of South Africa and South Madagascar, as they are near the Southern Ocean, where large swells are generated (Semedo *et al.* 2011). Apart from generating electricity, through turbines, wave energy can also be used to produce potable water via desalination, while seawater can be used as the feed water in the desalination plants (Abd-Elaty *et al.* 2022; Panagopoulos 2022a, 2022b), and, further, it can be used for water pumping for irrigation.

The Mozambique Channel, which is located in the south-western Indian Ocean, and oriented north-southwards, with two openings, one in the south and the other in the north (Figure 1), may be a suitable site for wave energy production, given the fact that the southern entrance of the channel is adjacent to the extratropical South Indian Ocean, part of the Southern Ocean, where large swell waves are generated, and the northern entrance is adjacent to the Tropical South Indian Ocean, another swell-generating area (Semedo *et al.* 2011; Lin & Oey 2020). The Mozambique Channel receives swell from both the south and northern entrances in addition to winds generated by the local trade and monsoon winds. The complex interaction of these waves may result in interference patterns, which could either increase or decrease the wave height (Sci. Behaviour of waves. Science Learning Hub 2011;

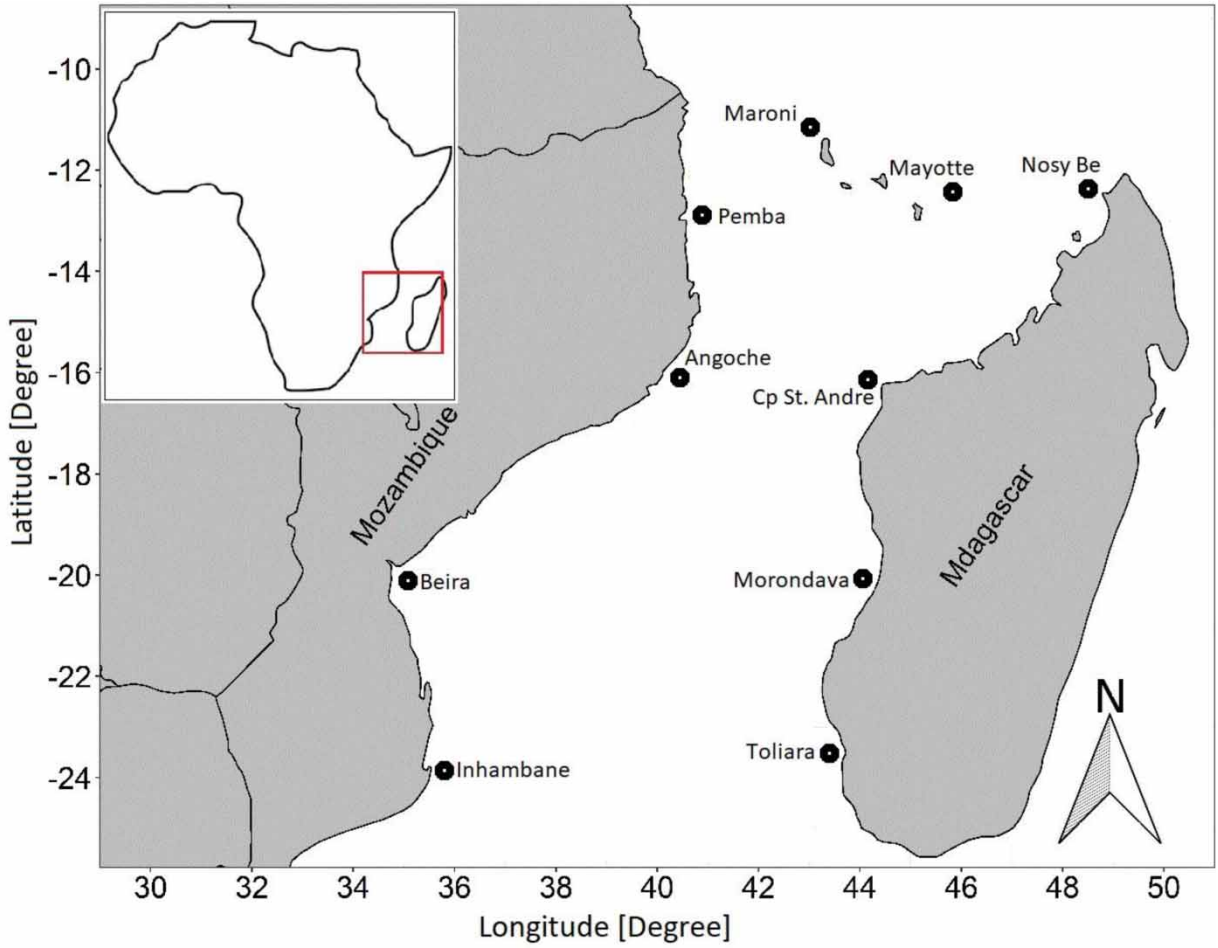

Figure 1 | Location of the study area.

Støle-Hentschel *et al.* 2020). There are few published studies on wave energy in the Mozambique Channel. Semedo *et al.* (2011) and Lin & Oey (2020) analysed ocean wave climatology on a global scale and dedicated a chapter to the Western Indian Ocean (WIO), and focussed on wave generation and propagation. Hammar *et al.* (2012) conducted studies on a number of ocean energy forms in the WIO, including the Mozambique Channel, but on a coarse spatial resolution, hence, less detail. None of the previous studies addressed the variability of wave energy in the study region.

The present paper examines in detail the near-shore wave energy potential in the Mozambique Channel, where the authors expect the occurrence of regions of very high waves as a result of the complex interaction of swell entering from both sides of the entrances and locally generated waves (Sci. Behaviour of waves. Science Learning Hub 2011; Støle-Hentschel *et al.* 2020). Wave energy potential and wave variability have been assessed at ten selected sites along the coast of Mozambique, Western Madagascar, and near the Comoro and Mayotte islands. Potential applications of available wave energy were discussed based on the wave energy density and variability. The present study contributes to the literature on wave energy near the coast of the Mozambique Channel and it is expected that the information presented in this paper will be useful to Government and other relevant organizations in making an informed decision with regard to major investments for harnessing the wave energy resource of the Mozambique Channel.

2. METHODOLOGY

2.1. Brief description of the study site

The Mozambique Channel is an open channel located in the WIO sub-region (Figure 1). The geographic limits of the Mozambique Channel are described by the International Hydrographic Organization (IHO 1953). The channels extend from about

10°S to 26°S. At the northern boundary, the channel is limited by the line joining the Rovuma estuary and the northern border of Mozambique, passing through the RasHabu Ile Grande Comore, on the Comoro archipelago, to the northern tip of the Madagascar Island. The southern limit is a line joining Cap Sainte-Marie, the southern end of Madagascar Island to Ponto do Ouro, the southern border of Mozambique. The eastern limit is Madagascar's west coast and the western limit is the Mozambique coast. The topography is well described by Breitzke *et al.* (2017). Its width varies from 400 to 950 km and it has a maximum depth of 3,292 m. There are two distinct seasons, the dry and cool winter season between March and August, and the wet and warm season from September to February (Barimalala *et al.* 2020). The circulation is dominated by anti-cyclonic and cyclonic me so-scale eddies, which transport warm water from the South Equatorial Current to the Agulhas Current in the south (Lutjeharms *et al.* 2012). The region is influenced by the trade winds and the northern part is also influenced by the seasonal north-eastern monsoon winds (Semedo *et al.* 2011). During the southern hemisphere winter, when the north-eastern monsoon occurs, the winds enter the channel from both directions, north and south (Semedo *et al.* 2011). The wave climatology is dominated by swells generated in the Southern Ocean and propagating northwards through the channel (Semedo *et al.* 2011), and swell waves generated by the northern winds, penetrate the channel from the northern boundary and propagate southwards (Semedo *et al.* 2011).

2.2. Data set

In this study, weekly data of daily averaged significant wave height and wave period, measured from satellite altimeters, provided by a marine-analyst (http://www.marine-analyst.eu), were used. The data cover the period from 29 June 2019 to 31 December 2021, in the selected quadrats in the Mozambique Channels, whose coordinates are given in Table 1 (see Figure 1 for further geographical locations).

Modern methods of ocean wave assessment are based on altimetry, with the height and period of waves determined from remote-sensing observations and calibrations using buoy measurements (Hammar *et al.* 2012). Indeed, altimetry data with higher spatial and temporal resolution was thought to generate more conservative estimates for the WIO coast (Hammar *et al.* 2012). Despite these advantages, there are two major drawbacks of remote-sensing methods, namely inaccuracy in near-shore waters (Krogstad & Barstow 1999; Cornett 2008a) and difficulties in fully accounting for the energy in ocean swell (Krogstad & Barstow 1999).

2.3. Wave power estimates

The wave power or wave energy flux per unit length of a crest (W m^{-1}) was calculated using the following equation (Semedo *et al.* 2011; Doorga *et al.* 2018):

$$P_W = \frac{\rho g^2}{64\pi} H_s^2 T_e \tag{1}$$

where P_W is the wave power, $\rho = 1{,}024$ kg m^{-3} is the density of sea water, $g = 9.81$ m s^{-2} is the acceleration due to gravity, H_s is the significant wave height in metres and T_e is the wave energy period given in seconds. The wave energy period is related to

Table 1 | Coordinates of the quadrats where the wave data were retrieved

		Latitude (°S)		Longitude (°E)	
Region	**Local**	**Initial**	**Final**	**Initial**	**Final**
Western side of the channel	Moroni	11.37	12.01	42.85	43.24
	Pemba	10.92	13.28	40.25	42.45
	Angoche	16.09	16.09	39.86	40.25
	Beira	18.96	20.92	34.61	37.24
	Inhambane	21.23	23.50	35.11	37.57
Eastern side of the channel	Mayotte	11.32	11.97	43.45	43.85
	Nosy Be	12.96	13.61	47.80	48.19
	Cape St. Andre	15.80	16.44	44.42	44.81
	Morondava	19.95	20.60	43.87	44.26
	Toliara	23.33	23.66	43.51	43.65

the peak wave period by the following formula, assuming a Pierson–Moskowitz wave spectrum shape (Sierra *et al.* 2016; Doorga *et al.* 2018):

$$T_e \approx 0.86 T_p \tag{2}$$

Combining Equations (1) and (2), and substituting the constants, the wave energy flux per metre of wave crest front length [kW m^{-1}] is given by Doorga *et al.* (2018):

$$P_W \approx 0.49 H_s^2 T_p \tag{3}$$

Besides estimating the wave energy potential at the sites, the temporal variability of the energy was also calculated. Steady wave energy fluxes are preferred to unsteady wave regimes due to the fact that they are more reliable and display greater efficiency, according to Rusu & Soares (2012).

Two coefficients that were proposed by Cornett (2008b) and applied by (Doorga *et al.* 2018) are employed to assess the temporal variability in wave power for selected sites around the island. They are the Coefficient of Variation (*CV*) and the Seasonal Variability Index (*SV*). The *CV* is obtained through the ratio of standard deviation (σ) of the wave power time series [$P(t)$ and the mean power (μ)]. A lower *CV* value is preferable to ease the sizing of a wave conversion system and to reduce the possible dumping of the converted wave energy. The *CV* is given by:

$$CV(P) = \frac{\sigma|f(t)|}{\mu|f(t)|} \tag{4}$$

The *SV* gives an indication of the seasonal variation that exists within the analysed time frame. It is obtained by subtracting the mean wave power for the highest ($P_{S(max)}$) and lowest ($P_{S(min)}$) energy seasons and dividing it by the annual mean wave power (P_{year}). The equation describing *SV* is given by (Doorga *et al.* 2018):

$$SV = \frac{P_{S(\max)} - P_{S(\min)}}{P_{year}} \tag{5}$$

Also of interest is the probability of occurrence of waves with characteristics above the threshold for viable energy harvesting. In the present work, threshold values of 1.6 m for significant wave height and energy flux of 10 kW m^{-1} were set, as used by Hammar *et al.* (2012) and Spaulding & Grilli (2010). The probability for the occurrence of waves above the critical level, assuming a Gaussian distribution, was determined by the following relationship (Jaynes 2003):

$$P(x > x_c) = 1 - \Phi\left(\frac{x_c - \mu}{\sigma}\right) \tag{6}$$

where x is the wave parameter, Φ is the probability density function of the standard normal distribution, x_c is the threshold or critical level, and μ and σ are the mean and standard deviation of the variable x, respectively.

3. RESULTS

3.1. Time series of wave properties and wave energy flux

Figures 2 and 3 present the time series of significant wave height, wave period, and wave energy flux at the selected sites near the coast in the western and eastern Mozambique Channel. On the western side of the Mozambique Channel (Figure 2), the significant wave height varied from about 0.5 m to about 5 $\pm$ 0.5 m, with the highest values observed in Inhambane, the most southern point studied. At this location, the average significant wave height was about 2 $\pm$ 0.7 m, followed by Beira with an average significant wave height of about 1.8 $\pm$ 0.6 m. The northern survey sites had an average significant wave height of about 1.3 $\pm$ 0.5 m. Swell heights peak at 4–4.5 $\pm$ 0.6 m during storms. There is a seasonal variation; in the southern hemisphere winter, which spans from April to October, wave heights were higher. The wave period ranged from about 4 to 14 $\pm$ 1.8 s, averaging at 4–5 $\pm$ 1.3 s, with no clear differences along the channel. The energy flux time series followed similar patterns to that of wave height, with values varying from about 1 to 85 $\pm$ 14.5 kW m^{-1}. The highest energy fluxes were recorded in Inhambane, averaging at 16 $\pm$ 9.4 kW m^{-1}, followed by Beira with an average of 11 $\pm$ 5.7 kW m^{-1}. The northern

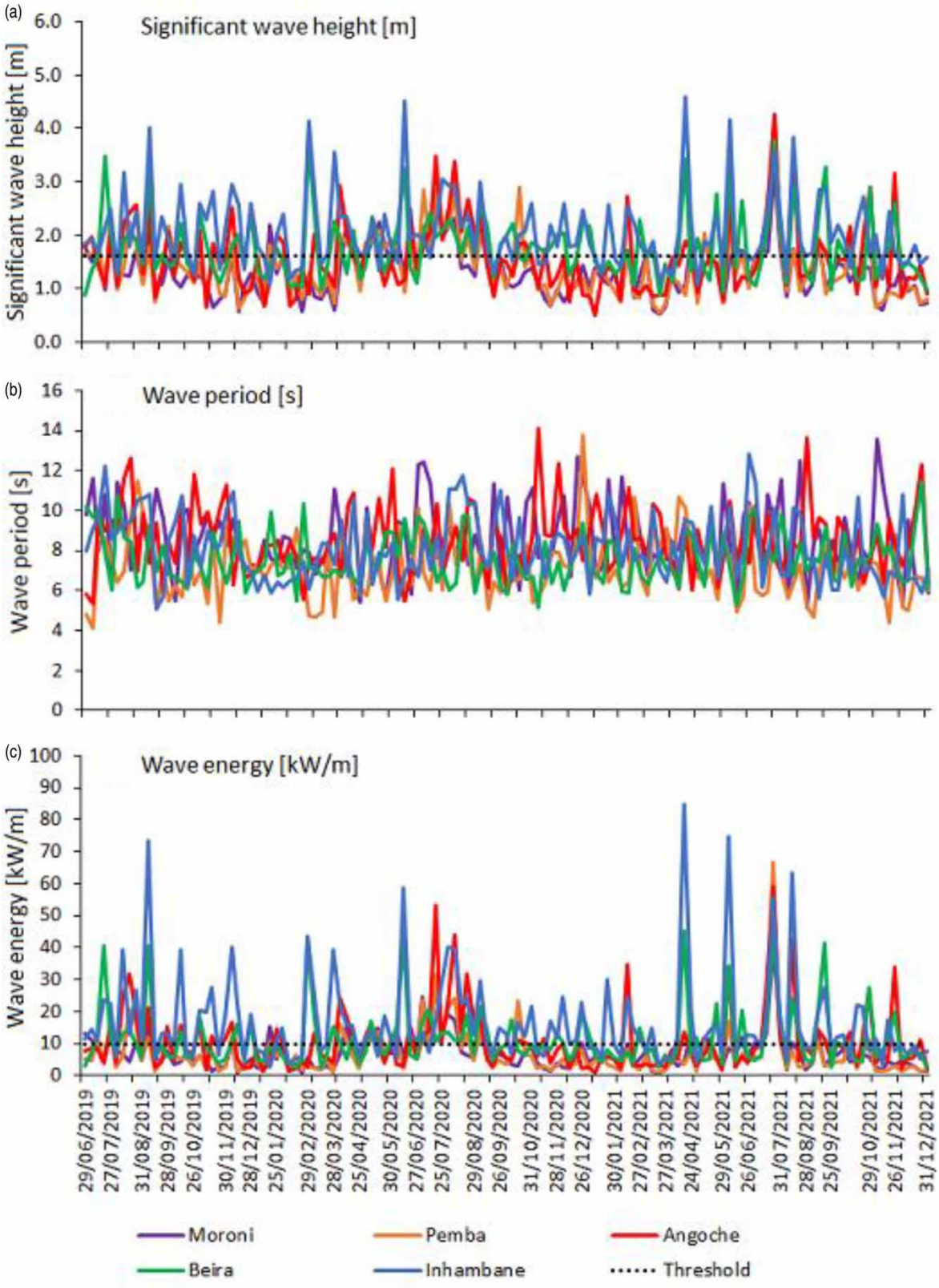

Figure 2 | Time series plots of significant wave height, wave period, and wave energy flux, near the coast, on the western side of the Mozambique Channel.

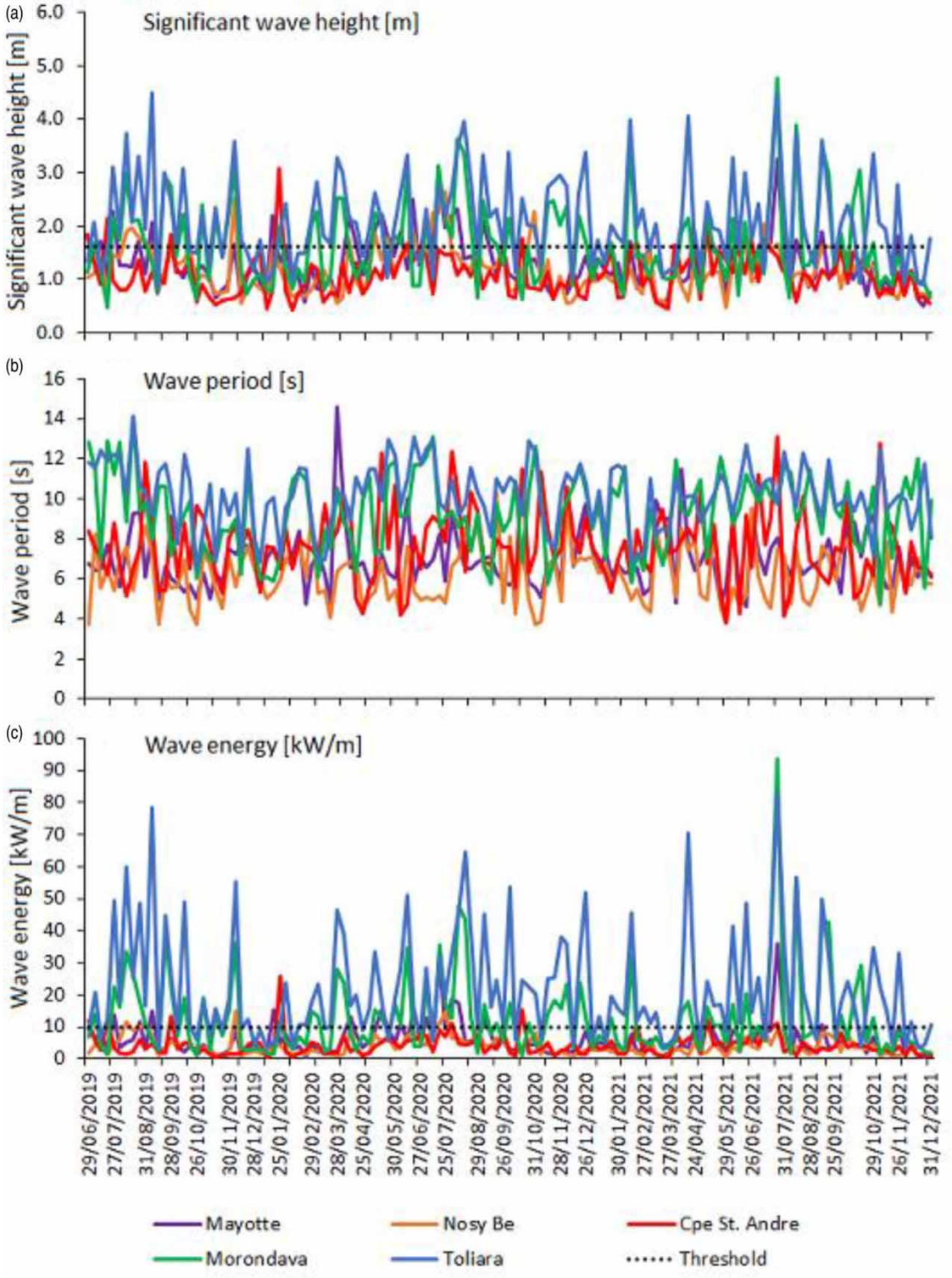

Figure 3 | Time series plot of significant wave height, wave period, and wave energy flux, near the cost, in the eastern side of the Mozambique Channel.

sites had an average of $6 \pm 3.5\ \mathrm{kW\ m^{-1}}$ each. The Inhambane and Beira sites exceeded on many occasions the minimum threshold of both the significant wave height (1.5 m) and energy flux ($10\ \mathrm{kW\ m^{-1}}$), making them the most suitable areas for the installation of wave energy extraction devices.

On the eastern side of the Mozambique Channel (Figure 3), the significant wave height varied from about 0.4 to 4.7 m, with the southernmost stations experiencing the largest waves. The average significant wave height at Toliara, the southernmost point, was 2.1 ± 0.8 m and at Morandavait was 1.7 ± 0.8 m, whereas at the northern stations the average significant wave height was 1.3 ± 0.5 m for Mayotte, 1.2 ± 0.4 m for Nosy Be, and 1.1 ± 0.4 m for Cape St. Andre. The wave period varied from about 3.7 ± 1.4 to 14.5 ± 1.7 s, with longer period waves observed in the southern part of the channel at Toliara, with an average wave period of about 10 ± 1.6 s and at Morondava with an average period of about 9 ± 1.7 s. At the northern stations, the average wave period was about 6–7 ± 1.4 s. The energy flux varied from 0.3 to 94 ± 17.2 kW m^{-1}, with the highest energy flux, observed at Toliara, the southernmost station, where the average was 23 ± 11.3 kW m^{-1}, followed by Morondava, where the average energy flux was 13 ± 3.5 kW m^{-1}. The average energy flux at the northern stations varied in the range 4.5–6 ± 2.9 kW m^{-1}, with the highest (6 ± 2.9 kW m^{-1}) observed at Mayotte. The significant wave heights were below the minimum threshold (1.5 m) in most cases, except at Toliara and Morondava, where there were long periods when the threshold was exceeded. There is also a seasonal signal here, with the highest waves in the southern hemisphere winter, which coincides with the Indian ocean South-West Monsoon. Again, the southern sites are the most suitable for the installation of wave energy extraction devices.

3.2. Frequency distribution of the waves

Figures 4 and 5 show the frequency distributions of significant wave height, fitted with a Gaussian distribution curve, near the coast on the western and eastern sides of the Mozambique Channel, respectively. On the western side of the channel (Figure 4), the distribution curves have a skewness of 1 at Moroni and a skewness of 1.4 at Inhambane. More frequent high waves were observed at Inhambane, the southernmost site, where the most commonly occurring waves had a significant wave height in the interval 1–2 m, with the mode at 1.7 m. At Moroniand Beira, the mode was 1.6 m, followed by Angoche and Pemba, with the mode at 1.4 and 1.3 m, respectively. On the eastern side of the channel (Figure 5), the frequency distributions of the significant wave height are moderately skewed, with skewness values around 0.7–1.1. Mayotte, Nosy be, and Cape St. Andre presented a single mode at about 1.3 m, whereas Morondava presented a bi-modal shape, with modes at 1.3 and 2.3 m and Toliara presented a widespread shape spanning from 0.9 to 4.7 m.

Figures 6 and 7 show the frequency distributions of the wave period, also fitted with a Gaussian distribution curve. On the western side of the channel (Figure 6), the distribution curves varied from nearly normal, with the skewness value of 0.4 at Moroniand 0.5 at Inhamabne, to moderately skewed, with skewness values of 0.6–0.8 at the other sites. The most commonly occurring waves had a wave period in the interval 7–9 s, with longer period waves (≥8 s) observed at the southern sites (Inhambane) up to Angoche. The mode at Pemba is 5.7 s, and at Moroni 7.1 s. On the eastern side of the channel (Figure 7), only Mayotte displayed a skewed curve, with a skewness of 1.6, the other sites displayed a quasi-normal distribution shape with skewness varying from −0.3 to 0.5. Moroni and Toliara, the southernmost and the northernmost sites, presented a single mode, at about 7 and 10.5 s for Mayotte and Toliara, respectively. The other sites presented multiple mode shapes, spanning from 5 to 12 s.

3.3. Significant wave height vs. wave period

The relationship between the significant wave height and the wave period gives an idea of the steepness of the wave. Figures 8 and 9 show scatter plots of the significant wave height and wave period at the selected sites in the western and eastern Mozambique Channel, respectively. On the western side of the channel (Figure 8), most of the waves had significant wave height and wave period in the range of 0.5–2 m and 5–14 s, respectively, suggesting low wave steepness. At Inhambane, Beira, and Angoche there were steeper waves with wave periods in the range of 5–7 s and wave heights up to 4–5 m. On the western side of the channel (Figure 9), Nosy Be and Cape St. Andre presented less steep waves, with wave periods in the range of 4–10 s and wave heights in the range of 0.5–1.8 m and 4–18 s and 0.5–1.8 m, respectively. The southern stations, Toliara and Morondava, experienced steeper waves, with wave periods in the range of 5–18 s and wave heights greater than 4 m.

3.4. Wave energy as a function of wave state

Figures 10 and 11 present contour plots of the wave energy with respect to significant wave height and wave period in the selected sites near the coast on the western and eastern sides of the Mozambique Channel, respectively. On the western side of the channel (Figure 10), the highest energy was observed at Inhambane, the southernmost site, where the most energetic waves(≥50 ± 14.5 kW m^{-1}) occurred for significant wave heights equal to or greater than 3.5 m and a wave period of 10 ± 1.8 s. Pemba and Angoche experienced the highest energy (≥30 ± 5.7 kW m^{-1}) at significant wave heights equal to or greater than 2.5 m and wave periods in the interval 9–10 ± 1.8 s, whereas at Moroni and Beira the energy

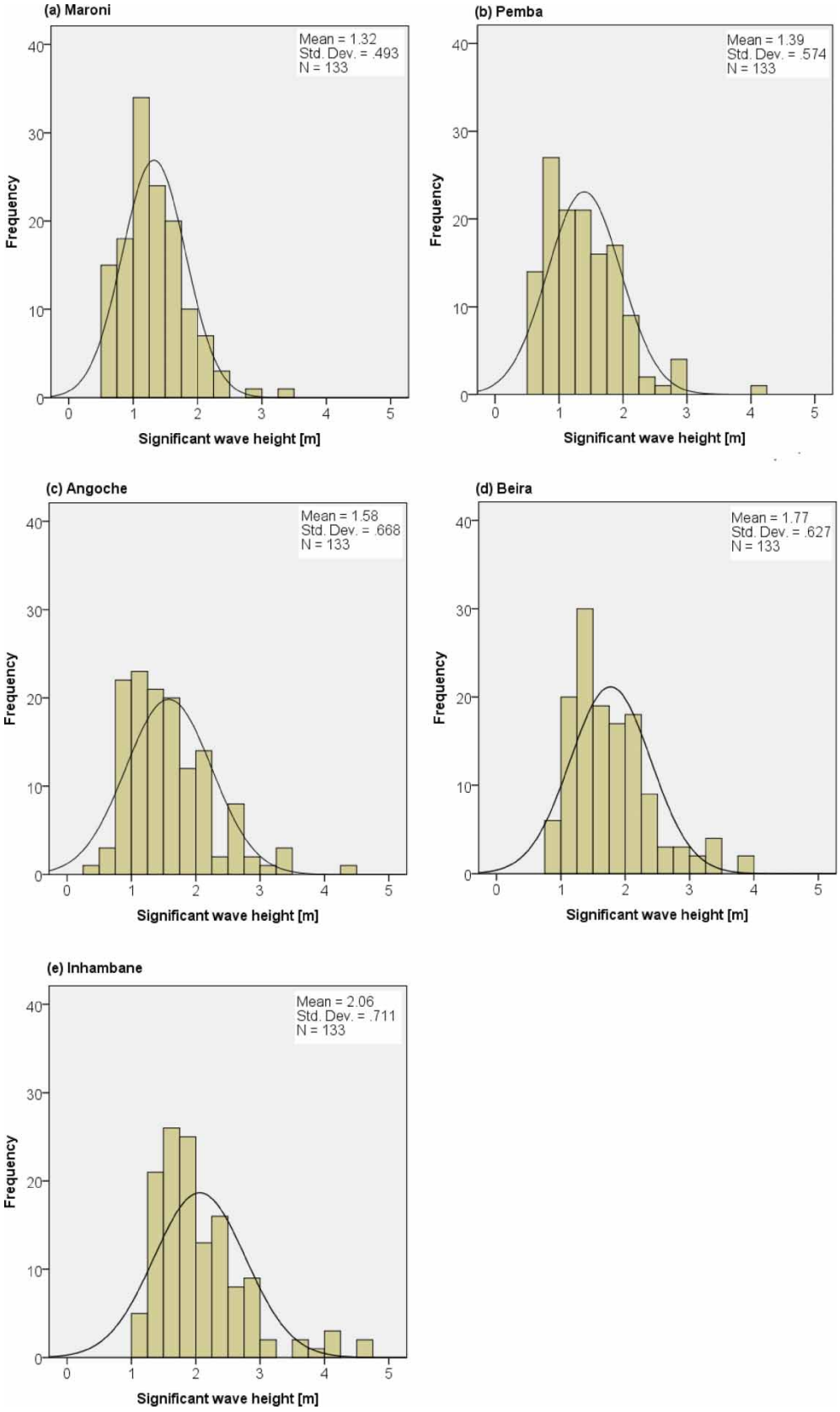

Figure 4 | Frequency distribution of the significant wave height on the western side of the Mozambique Channel.

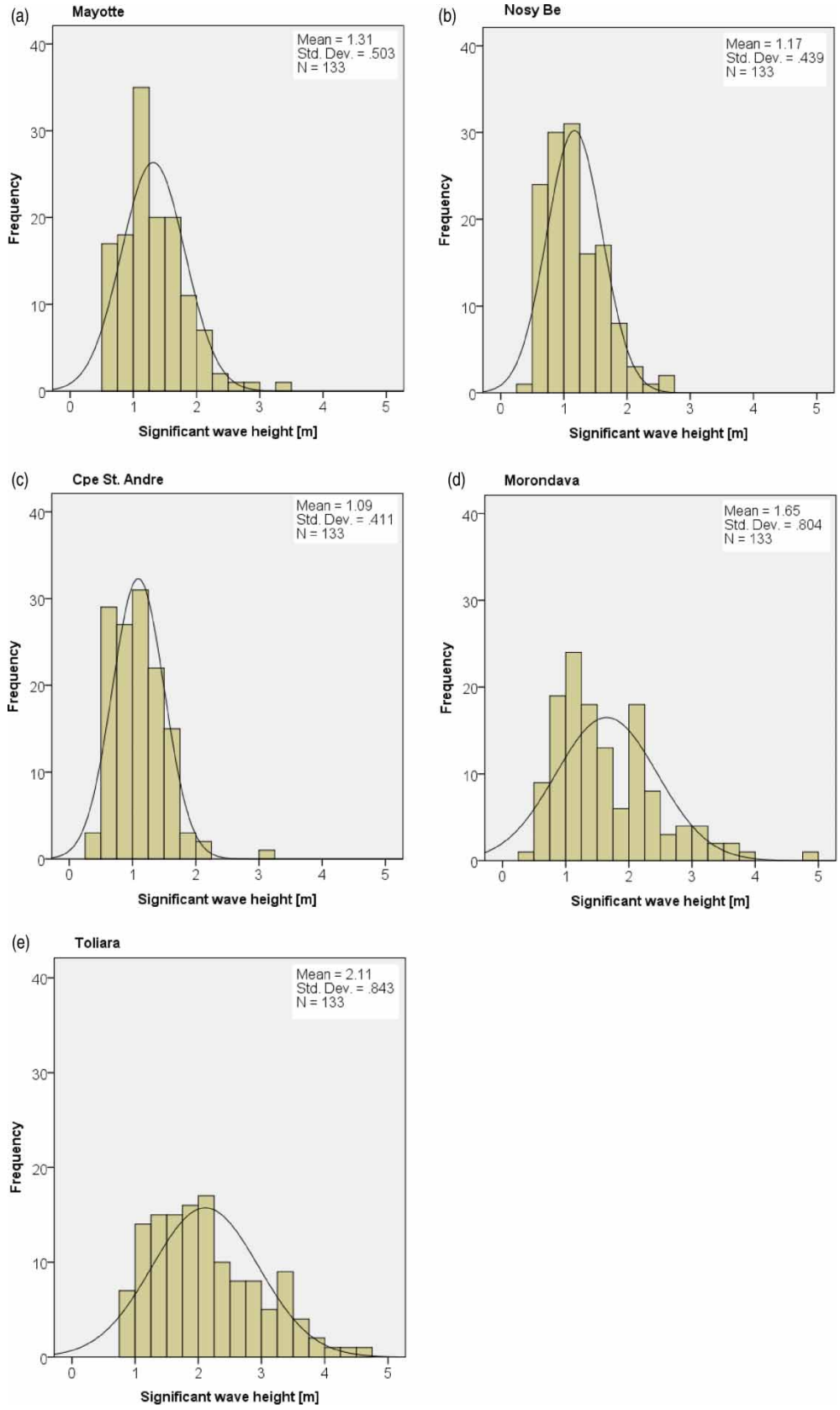

Figure 5 | Frequency distribution of the significant wave height on the eastern side of the Mozambique Channel.

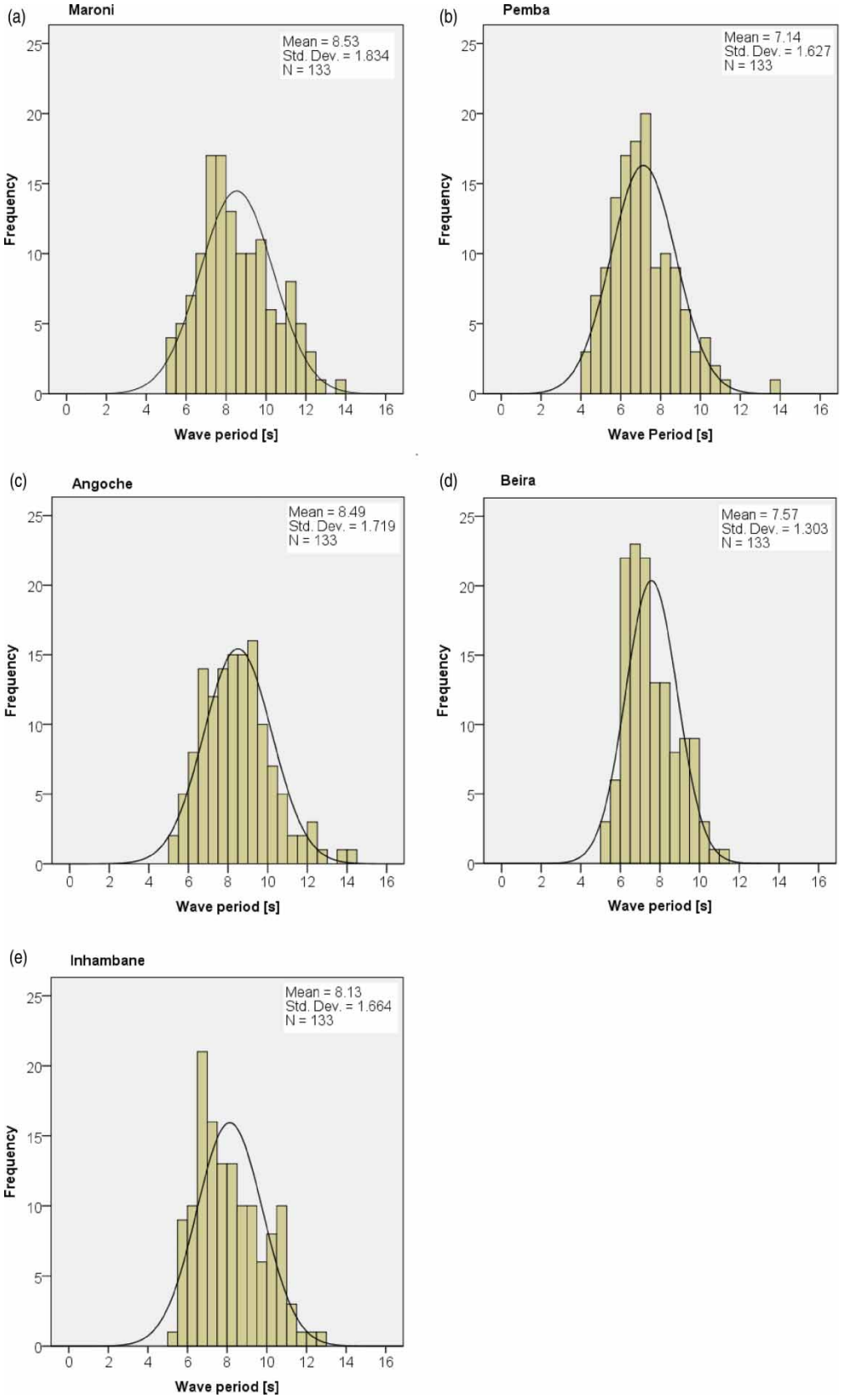

Figure 6 | Frequency distribution of the wave period at the western side of the Mozambique Channel.

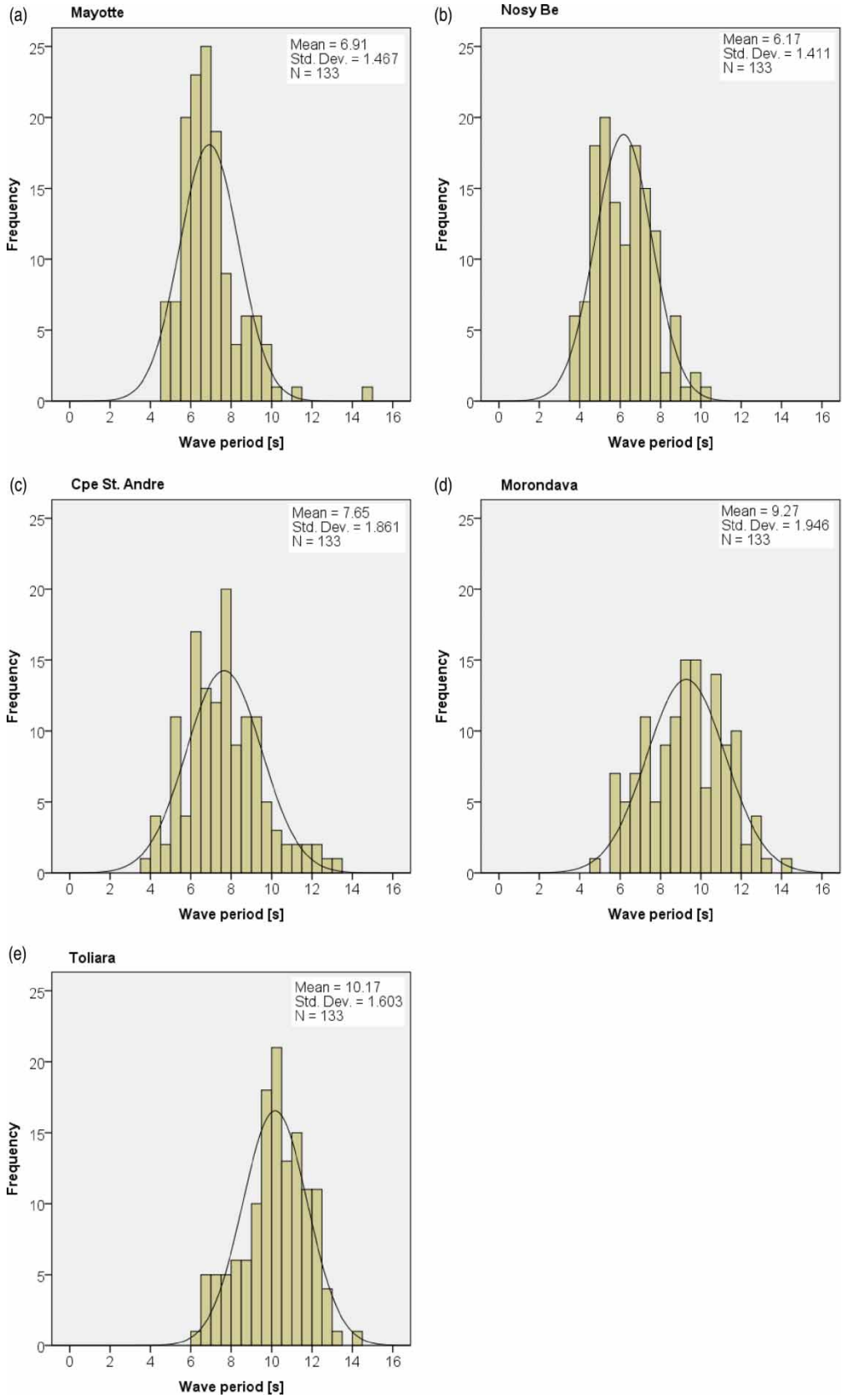

Figure 7 | Frequency distribution of the wave period at the eastern side of the Mozambique Channel.

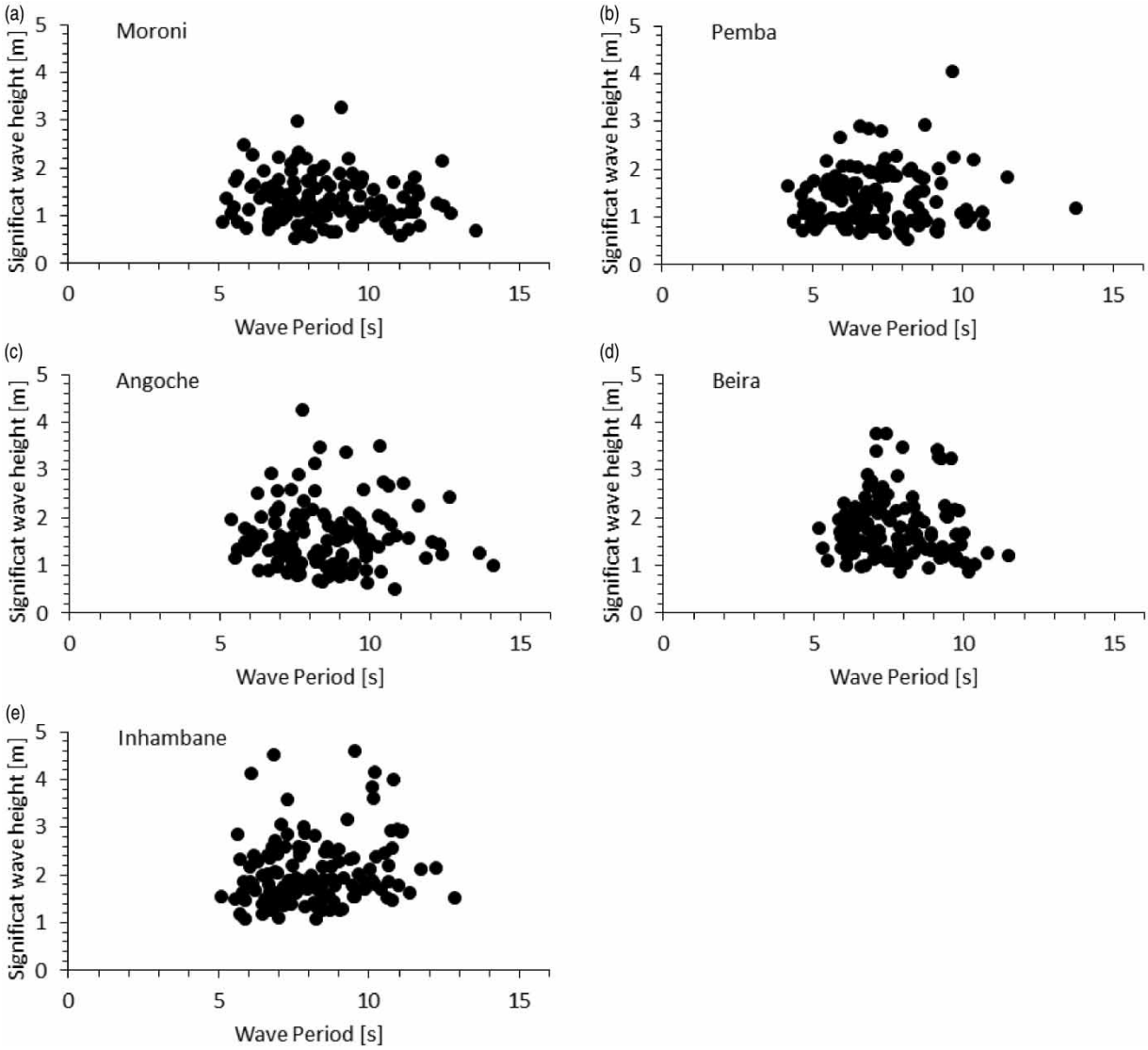

Figure 8 | Scatter plot diagram of significant wave height and wave period on the western side of the Mozambique Channel.

peaked ((≥25 ± 5.7 kW m^{-1}) also at significant wave heights equal to or greater than 2.5 m but at wave periods in the interval 10–11 ± 1.8 s. On the eastern side of the channel (Figure 11), energetic waves were also recorded at Morondava and Toliara, the southernmost sites, with energy peaking from 30 ± 5.7 up to 70 ± 14.5 kW m^{-1} and up to 55 ± 13.5 kW m^{-1}, respectively, and at the significant wave height in the interval 1.5–3 ± 0.5 m and wave period 10–11 ± 1.7 s, followed by Mayotte, the northernmost site, with energy in the interval 10–30 ± 5.2 kW m^{-1}, at the significant wave height of about 1.5 ± 0.5 m and wave period of about 10 ± 1.8 s. Low energetic waves were observed at Nose (5–10 ± 2.9 kW m^{-1}) and Cape St. Andre (10–15 ± 2.9 kW m^{-1}), with energy peaking at 1.2–1.5 ± 0.5 m significant wave height and wave period 6–10 ± 1.8 s.

An understanding of the performance of wave energy converters in different wave states is essential for the constructional details, cost, and efficiency of the installed device. It would be preferable to install a wave energy converter in wave conditions having a maximum total energy flux rather than in one having maximum occurrence.

3.5. Wave variability and summary of wave statistics

Tables 2–4 present the summary statistics of the wave characteristics and wave energy near the coast in the western and eastern Mozambique Channel. From Table 2, it can be seen clearly that the southern Mozambique Channel experiences the highest waves on both sides of the channel (1.7–2.1 m, on average). The northern part of the channel experiences lower

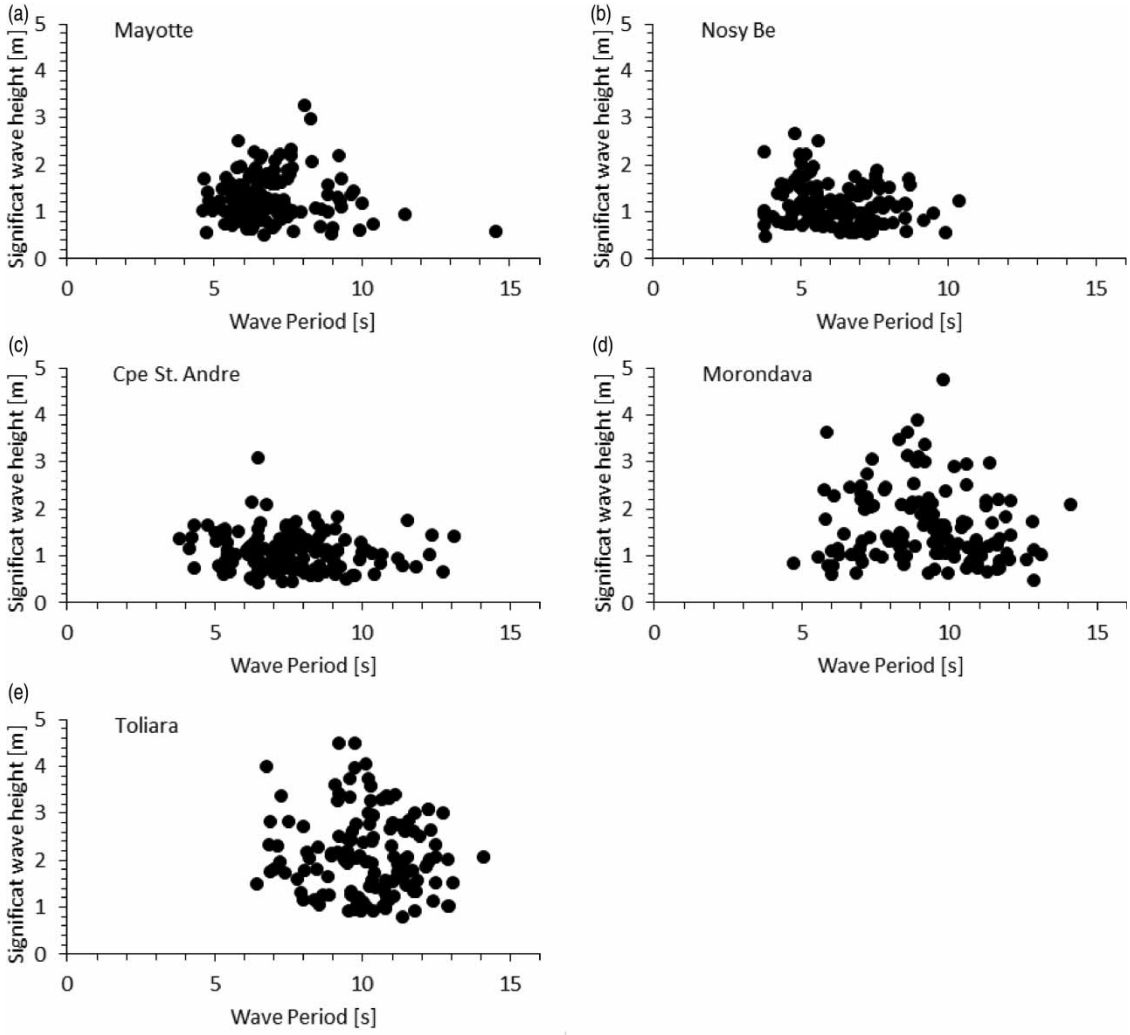

Figure 9 | Scatter plot diagram of significant wave height and wave period on the eastern side of the Mozambique Channel.

waves (1.2–1.4 m). The probability of the significant wave height attaining and exceeding the minimum threshold values (1.6 m) averages 63% on the western side against 62% on the eastern side. This is considered a marginal difference, though. Both sides of the channel displayed high variability of 34–47% and seasonal variability (1.6–2.5). From Table 3, summary statistics for the wave period, it can be seen that large swell waves were recorded in the southern part of the channel, where the largest (10 s on average) were recorded on the western side, followed by the northern site with an average period of 8.5 s in the western side. The variability in wave period was low (15–24%) and the seasonal variability was also low (1.0–1.4) compared with the variability of the significant wave height. From Table 4, referring to energy flux, it can be seen that the most energetic waves (11–23 $\pm$ 4.5 kW m^{-1}) were encountered in the southern part of the channel, with the highest energy (13–23 $\pm$ 4.5 kW m^{-1}, on average) observed in the eastern part of the channel. In the northern part of the channel, the energy averaged to 4–7 $\pm$2.5 kW m^{-1}. The variability of the wave energy was highest on the western side of the channel (80–108%) compared with the eastern side (71–99%). However, the probability of the energy flux attaining and exceeding the threshold value (10 $\pm$ 2.5 kW m^{-1}) was higher on the western side, averaging 63%, compared to the eastern side where it averaged 61%.

4. DISCUSSION

4.1. Spatio-temporal distribution of wave energy patterns

The results of the present study showed clearly that the highest significant wave heights, and hence, the most energetic waves, given the close correlation between the significant wave height and wave energy flux, were observed in the southern part of

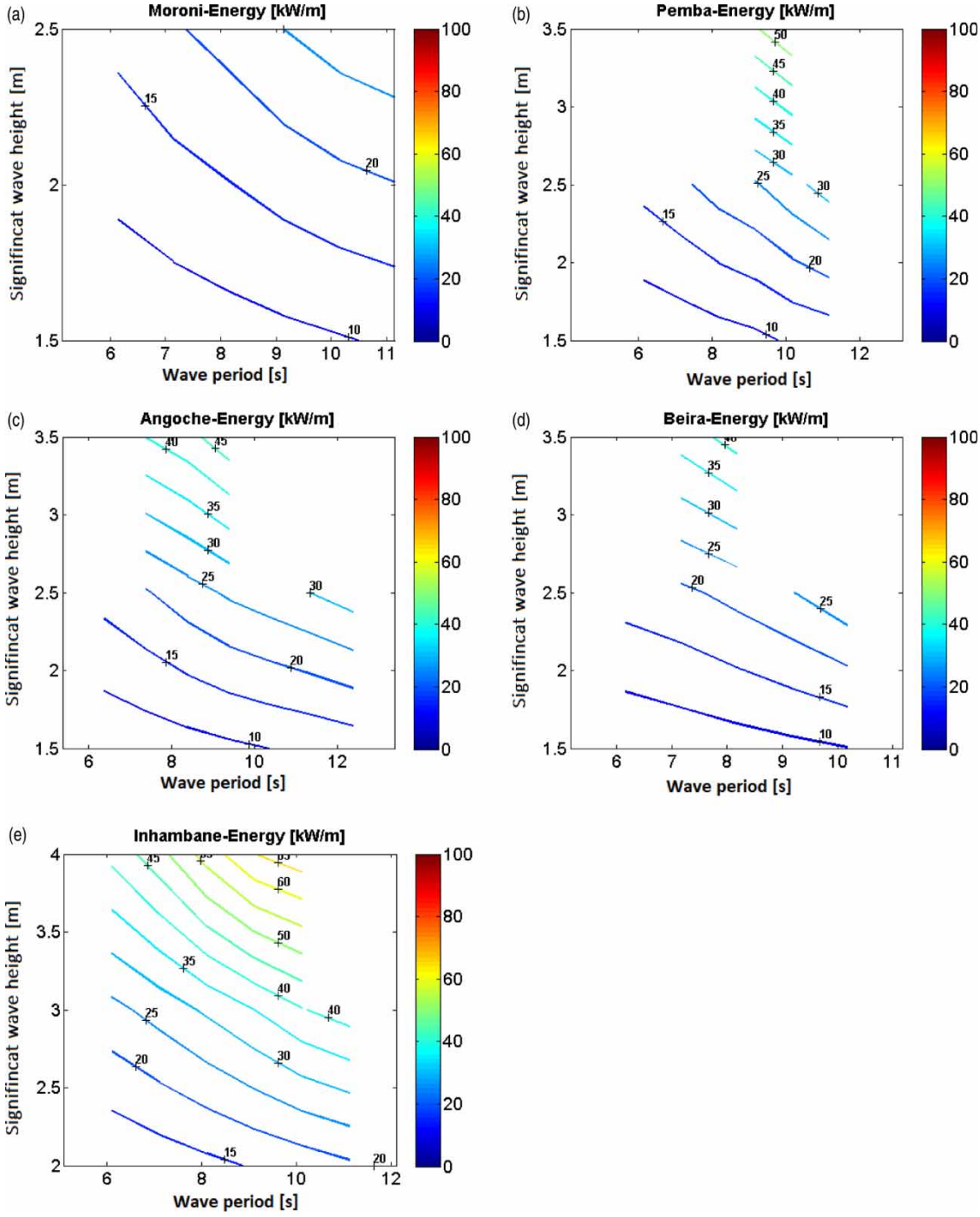

Figure 10 | Contour plots of wave energy as a function of significant wave height and wave period on the western side of the Mozambique Channel.

the channel. Here, significant wave heights reached 4.5 ± 0.7 m and averaged to about 2 ± 0.5 m. Wave energy flux averaged at 16–22 ± 5.6 kW m^{-1} at Inhambane and Toliara, the southernmost sites studied. The northern opening of the channel was also characterized by relatively high energetic waves with an average significant wave height in the range 1.3–1.4 ± 0.5 m and attaining maxima of 3–4 ± 0.5 m. The energy flux is in the range of 7.0–10.5 ± 5.6 kW m^{-1} on average peaking at 40–66 ± 9.3 kW m^{-1}.

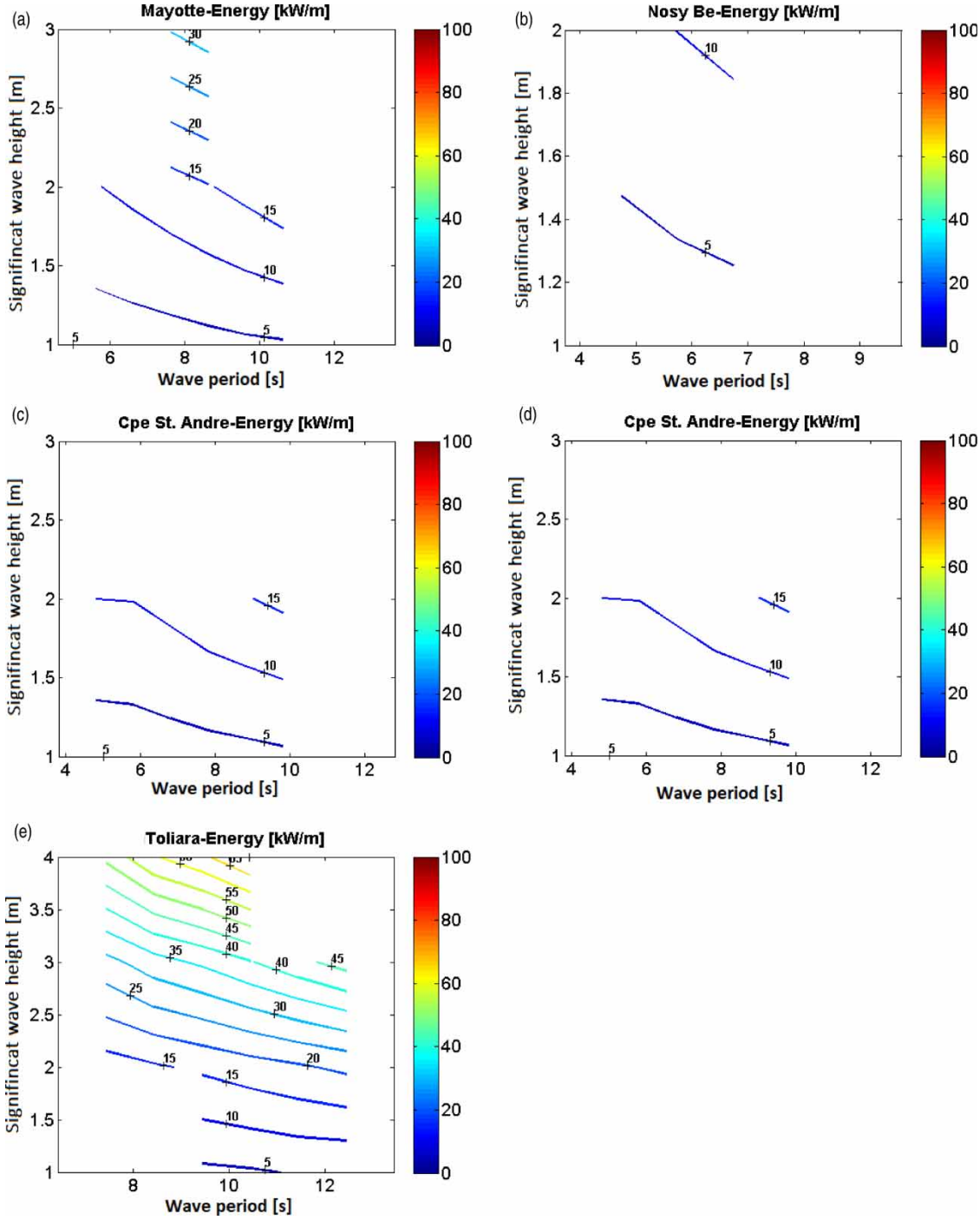

Figure 11 | Contour plots of wave energy as a function of significant wave height and wave period on the eastern side of the Mozambique Channel.

These results are consistent with the findings of previous studies about wave climatology on a global scale (Semedo *et al.* 2011; Panagopoulos 2022a) and specifically for the WIO (Hammar *et al.* 2012). The high-energy waves in the southern part of the channel are attributed to swell from the Extratropical South Indian Ocean (Semedo *et al.* 2011; Lin & Oey 2020; Colosi *et al.* 2021; Rossi *et al.* 2021), whereas those observed in the northern part of the channel are attributed to swell generated in the Tropical South Indian Ocean region (Semedo *et al.* 2011; Hammar *et al.* 2012).

Table 2 | Summary of statistics of significant wave height near the coast of the Mozambique Channel

Region	Site	Average [m]	Min [m]	Max [m]	Standard deviation [m]	Mode [m]	Probability for $Hs \geq 1.5$ m [%]	*CV* [%]	*SV*	Skewness
Western side	Moroni	1.3	0.5	3.3	0.5	1.6	63	37.3	2.1	1.0
	Pemba	1.4	0.5	4.0	0.6	1.3	63	41.2	2.5	1.3
	Angoche	1.6	0.5	4.3	0.7	1.4	63	42.3	2.4	1.2
	Beira	1.8	0.9	3.8	0.6	1.6	63	35.4	1.6	1.2
	Inhambane	2.1	1.1	4.6	0.7	1.7	62	34.5	1.7	1.4
Eastern side	Mayotte	1.4	0.5	3.3	0.5	1.3	63	37.2	2.0	0.9
	Nosy Be	1.2	0.5	2.7	0.4	1.3	62	36.8	1.8	0.9
	Cape St. Andre	1.1	0.4	3.1	0.4	1.3	61	37.0	2.4	1.1
	Morondava	1.7	0.5	4.8	0.8	–	63	47.7	2.5	1.1
	Toliara	2.1	0.8	4.5	0.8	2.3	62	39.2	1.7	0.7

Table 3 | Summary of statistics of wave period near the coast of the Mozambique Channel

Region	Site	Average [s]	Min [s]	Max [s]	Standard deviation [s]	Mode [s]	*CV* [%]	*SV*	Skewness
Western side	Moroni	8.5	5.1	13.6	1.8	7.1	21.5	1.0	0.4
	Pemba	7.1	4.2	13.8	1.6	5.7	22.8	1.3	0.8
	Angoche	8.5	5.4	14.1	1.7	8.1	20.2	1.0	0.7
	Beira	7.6	5.2	11.5	1.3	8.9	17.2	0.8	0.6
	Inhambane	8.1	5.1	12.8	1.7	8.5	20.5	1.0	0.5
Eastern side	Mayotte	6.9	4.6	14.5	1.5	–	21.3	1.4	1.6
	Nosy Be	6.2	3.7	10.3	1.4	3.7	22.8	1.1	0.4
	Cape St. Andre	7.7	3.8	13.1	1.9	6.5	24.2	1.2	0.5
	Morondava	9.3	4.7	14.1	1.9	–	20.9	1.0	−0.1
	Toliara	10.2	6.4	14.1	1.6	–	15.7	0.8	−0.3

Table 4 | Summary of statistics of wave energy flux near the coast of the Mozambique Channel

Region	Site	Average [kW m^{-1}]	Min [kW m^{-1}]	Max [kW m^{-1}]	Standard deviation [kW m^{-1}]	Mode [kW m^{-1}]	Probability of energy ≥ 10 kW m^{-1}	*CV* [%]	*SV*	Skewness
Western side	Moroni	7.0	0.9	40.8	5.6	–	62	80.2	5.7	–
	Pemba	7.0	1.0	66.7	7.6	–	63	108.8	9.4	–
	Angoche	10.5	1.1	59.1	10.1	–	63	96.2	5.5	–
	Beira	11.3	2.5	45.0	9.3	–	63	82.3	3.8	–
	Inhambane	16.7	2.8	84.9	14.5	–	63	86.6	4.9	–
Eastern side	Mayotte	6.1	0.6	36.1	5.2	–	62	853	5.8	–
	Nosy Be	4.1	0.3	15.0	2.9	–	60	71.2	3.6	–
	Cape St. Andre	4.5	0.5	257	3.5	–	60	78.2	5.7	–
	Morondava	13.4	1.0	93.6	23.2	–	63	98.7	6.9	–
	Toliara	22.7	3.0	82.5	17.2	–	62	75.7	3.5	–

The central part of the channel was characterized by relatively low-energy waves, probably due to the fact that this region is less exposed to swell. However, in the western central part of the Mozambique Channel, on the Mozambique coast, large waves are observed. These have an average significant wave height in the range of 1.6–1.8 $\pm$ 0.5 m. The significant wave height here reaches a maximum of 3.8–4.3 $\pm$ 0.8 m and the average wave energy flux is 10.5–11.3 $\pm$ 5.6 kW m^{-1} at Angoche

and Beira, compared to values of 1 m and 4.5 ± 0.8 kW m^{-1} for Cape St. Andre on the central-eastern side of the channel. There was no evidence of larger waves resulting from constructive interference of waves inside the channel. The increase in wave height and wave energy on the western side of the channel may be attributed to Kelvin waves (Griffiths 2013).

The wave patterns in the whole of the Mozambique Channel exhibited a seasonal cycle, with large waves occurring during the time of the southern monsoon, during the southern hemisphere winter, as can be seen in the time series plots (Figures 2 and 3). This result is consistent with previous studies by Colosi *et al.* (2021), who attributed the observed high waves in the winter to seasonal changes in high-latitude storm patterns that generate swell which propagates equatorward.

4.2. Wave power variability and sustainability threshold

The waves in the Mozambique Channel are highly variable with a proportion of the variability of 34–47% for significant wave height and over 70% for wave energy. This high variability may be attributed to the effect of storms and cyclones which frequently affect the region (Matyas 2015; Muthige *et al.* 2018). High variability may affect the sustainability of any wave energy exploitation device (Rusu & Soares 2012). However, the thresholds for the viable exploitation of waves for energy production of 1.5 m for significant wave height and 10 kW m^{-1} for energy flux, are exceeded most of the time in the southern Mozambique Channel. This means that, though there is high wave variability, there is usually sufficient power to generate electricity and the southern part of the channel is suitable for wave energy harvesting for electricity production. On the western central and northern parts of the Mozambique Channel, the thresholds are exceeded from July to November, making these sites suitable for seasonal electricity production.

4.3. Wave power available and applications

There are many applications of wave energy, including electricity generation, water desalination, and pumping of water. Concerning electricity production, the threshold for technical and economic viability is set based on the converter devices. Wave exploitation for electricity production is recommended in areas with wave energy density $\geq 25 \pm 5.6$ kW m^{-1} (Lavidas & Blok 2021). It has been argued that moderate wave resources ($<25 \pm 5.6$ kW m^{-1}) may be economically viable if an optimal device is employed (Lavidas & Blok 2021). The threshold of 10 kW m^{-1} chosen in this study, based on Hammar *et al.* (2012), would assure sustainable electricity production in the southern part of the channel. But, based on the argument by Lavidas & Blok (2021), we recommend the development of appropriate devices for harvesting wave energy for electricity production in the western central Mozambique Channel, where the energy density is about the average for the world ocean (Colosi *et al.* 2021). Furthermore, the whole coastline of the Mozambique Channel has wave energy potential for water desalination as stated by Abd-Elaty *et al.* (2022) and further argued by Panagopoulos (2022a, 2022b) and for water pumping for irrigation, as these applications are the least demanding in terms of energy power and variability. Both desalination and irrigation would have a significant positive impact on the livelihood of people living in coastal areas and on coastal area development in the region, considering the fact that more than half of the population of the region lives in coastal areas (Taylor *et al.* 2019).

5. CONCLUDING REMARKS AND RECOMMENDATIONS

This study was based on averaged data over space and time, and therefore, the results must be interpreted with caution. The wave and wave energy climate near the coast of the Mozambique Channel are highly variable, changing as storms and cyclones pass through the area. However, the minimum threshold of significant wave height (1.5 m) and wave energy flux (10 kW m^{-1}) for electricity production is exceeded most of the time in the southern part of the channel. The southern winter is the time for the highest waves and greatest energy, and is, therefore, the most promising season for the deployment of wave energy harvesting devices. Although one should interpret with caution, the finding in this study suggests that the whole coast of Mozambique Channel is suitable for applications of wave energy resources for desalination and water pumping, with the potential to enhance the livelihood of more than half of the population of the region. The present study recommends studies on the development of appropriate wave energy harvesting devices for electricity production to match the power available in the central western and northern Mozambique Channel, where the energy density is at the level of the world ocean average. Further studies should be directed towards the exploitation of applications of the available wave resources for coastal development.

ACKNOWLEDGEMENTS

The research was part of PhD studies on renewable energy, financially supported by the Eduardo Mondlane University post-graduate research grant, under the SIDA-SAREC Project No 2.1.6. Thanks, are also due to Mrs Faith Bowers and Prof. D.G. Bowers for the constructive remarks and suggestions, which significantly improved the quality of the manuscript.

DATA AVAILABILITY STATEMENT

All relevant data are included in the paper or its Supplementary Information.

CONFLICT OF INTEREST

The authors declare there is no conflict.

REFERENCES

Abd-Elaty, I., Kushwaha, N. L., Grismer, M. E., Elbeltagi, A. & Alban Kuriqi, A. 2022 Cost-effective management measures for coastal aquifers affected by saltwater intrusion and climate change. *Science of The Total Environment* **836**, 155656. https://doi.org/10.1016/j.scitotenv.2022.155656.

Barimalala, R., Blamey, R. C., Desbiolles, F. & Reason, C. J. C. 2020 Variability in the Mozambique channel trough and impacts on Southeast African rainfall. *Journal of Climate* **33**, 749–765. doi:10.1175/JCLI-D-19-0267.1.

Breitzke, M., Wiles, E., Krocker, R., Watkeys, M. K. & Jokat, W. 2017 Seafloor morphology in the Mozambique channel: evidence for long-term persistent bottom-current flow and deep-reaching eddy activity. *Marine Geophysical Research* **38**, 241–269. https://doi.org/10.1007/s11001-017-9322-7.

Colosi, L. V., Villas Bôas, A. B. & Gille, S. T. 2021 The seasonal cycle of significant wave height in the ocean: local versus remote forcing. *Journal of Geophysical Research: Oceans* **126** (8), e2021JC017198. https://doi.org/10.1029/2021JC017198.

Cornett, A. M. A. 2008a Global wave energy resource assessment. Ottawa: Canadian Hydraulic Centre. In: *The Proceedings of the Eighteenth (2008) International Offshore and Polar Engineering Conference*, July 6–11, 2008, Vancouver, Canada. Paper No. ISOPE-2008-TPC-579.

Cornett, A. M. 2008b A Global wave energy resource assessment. In *The Eighteenth International Offshore and Polar Engineering Conference*. International Society of Offshore and Polar Engineers.

Deichmann, U., Meisner, C., Murray, S. & Wheeler, D. 2011 The economics of renewable energy expansion in rural sub-Saharan Africa. *Energy Policy* **39** (1), 215–227. https://doi.org/10.1016/j.enpol.2010.09.034.

Doorga, J. R. S., Chinta, D., Gooroochurn, O., Rawat, A., Ramchandur, V., Motah, B. A., Sunassee, S. & Samyan, C. 2018 Assessment of the wave potential at selected hydrology and coastal environments around a tropical island, case study: Mauritius. *International Journal of Energy and Environmental Engineering* **9**, 135–153. https://doi.org/10.1007/s40095-018-0259-7.

ESI Africa, South Africa: wave energy power plant development. 2015 Available from: https://www.esi-africa.com/top-stories/south-africa-wave-energy-power-plant-development/

Griffiths, S. D. 2013 Kelvin wave propagation along straight boundaries in C-grid finite-difference models. *Journal of Computational Physics* **255**, 639–659. doi:10.1016/j.jcp.2013.08.040.

Hafner, M., Tagliapietra, S. & de Strasser, L. 2018 Prospects for renewable energy in Africa. In: *Energy in Africa*. Springer Briefs in Energy, Springer, Cham, pp. 47–75. https://doi.org/10.1007/978-3-319-92219-5_3.

Hammar, L., Ehnberg, J., Mavume, A., Cuamba, B. C. & Molander, S. 2012 Renewable ocean energy in the Western Indian Ocean. *Renewable and Sustainable Energy Reviews* **16** (7), 4938–4950. https://doi.org/10.1016/j.rser.2012.04.026.

IHO 1953 *Limits of Oceans and Seas*, 3rd edn. IHO Special Publication, 23. International Hydrographic Organization (IHO), Monaco, p. 38. Available from: http://marineregions.org/mrgid/4261. (accessed 31 July 2022).

Jaynes, E. T. 2003 *Probability Theory: The Logic of Science*. Cambridge University Press, St. Louis, MO, USA, pp. 592–593. ISBN 9780521592710.

Krogstad, H. E. & Barstow, S. F. 1999 Satellite wave measurements for coastal engineering applications. *Coastal Engineering* **37**, 283–307.

Lavidas, G. & Blok, K. 2021 Shifting wave energy perceptions: the case for wave energy converter (WEC) feasibility at milder resources. **170**, 1143–1155. https://doi.org/10.1016/j.renene.2021.02.041.

Lin, Y. & Oey, L. 2020 Global trends of Sea surface gravity wave, wind, and coastal wave setup. *Journal of Climate* **33** (3), 769–785. Available from: https://journals.ametsoc.org/view/journals/clim/33/3/jcli-d-19-0347.1.xml. (accessed 6 October 2021).

Lutjeharms, J. R. E., Biastoch, A., Van der Werf, P. M., Ridderinkhof, H. & De Ruijter, W. P. M. 2012 On the discontinuous nature of the Mozambique current. *South African Journal of Science* **108** (1/2), 5. Art. #428. http://dx.doi.org/10.4102/sajs.v108i1/2.428.

Matyas, C. J. 2015 Tropical cyclone formation and motion in the Mozambique channel. *International Journal of Climatology* **35** (3), 375–390. doi:10.1002/joc.3985.

Muthige, M. S., Malherbe, J., Englebrecht, F. A., Grab, S., Beraki, A., Maisha, T. R. & Van der Merwe, J. 2018 Projected changes in tropical cyclones over the south west Indian ocean under different extents of global warming. *Environmental Research Letters* **13** (6), 065019. https://doi.org/10.1088/1748-9326/aabc60.

Ouedraogo, N. S. 2017 Africa energy future: alternative scenarios and their implications for sustainable development strategies. *Energy Policy* **106**, 457–471. http://dx.doi.org/10.1016/j.enpol.2017.03.021.

Owusu, P. A. & Asumadu-Sarkodie, S. 2016 A review of renewable energy sources, sustainability issues and climate change mitigation. *Cogent Engineering* **3** (1), 1167990. https://doi.org/10.1080/23311916.2016.1167990.

Panagopoulos, A. 2022a Brine management (saline water & wastewater effluents): sustainable utilization and resource recovery strategy through Minimal and Zero Liquid Discharge (MLD & ZLD) desalination systems. *Chemical Engineering and Processing – Process Intensification*, 108944. https://doi.org/10.1016/j.cep.2022.108944.

Panagopoulos, A. 2022b Process simulation and analysis of high-pressure reverse osmosis (HPRO) in the treatment and utilization of desalination brine (saline wastewater). *International Journal of Energy Research*. https://doi.org/10.1002/er.8607.

Rossi, G. B., Cannata, A., Iengo, A., Migliaccio, M., Nardone, G., Piscopo, V. & Zambianchi, E. 2021 Measurement of Sea waves. *Sensors (Basel)* **22** (1), 78. doi:10.3390/s22010078. PMID: 35009617; PMCID: PMC8747634.

Rusu, E. & Soares, C. G. 2012 Wave energy pattern around the Madeira islands. *Energy* **45** (1), 771–785.

Sci. Behaviour of waves. Science Learning Hub. 2011 Available from: https://www.sciencelearn.org.nz/resources/121-behaviour-of-waves. (accessed 30 September 2021).

Semedo, A., Sušelj, K., Rutgersson, A. & Sterl, A. 2011 A global view on the wind Sea and swell climate and variability from ERA-40. *Journal of Climate* **24** (5), 1461–1479. doi:10.1175/2010JCLI3718.1.

Sierra, J. P., Martn, C., Msso, C., Mestres, M. & Jebbad, R. 2016 Wave energy potential along the Atlantic coast of Morocco. *Renewable Energy* **96**, 20–32. doi:10.1016/j.renene.2016.04.071.

Spaulding, M. L. & Grilli, A. 2010 Application of technology development index and principal component analysis and cluster methods to ocean renewable energy facility siting. *Marine Technology Society Journal* **44**, 8–23.

Støle-Hentschel, S., Trulsen, K., Nieto Borge, J. C. & Olluri, S. 2020 Extreme wave statistics in combined and partitioned windsea and swell. *Water Waves* **2**, 169–184. https://doi.org/10.1007/s42286-020-00026-w.

Taylor, S. F. W., Roberts, M. J., Milligan, B. & Ncwadi, R. 2019 Measurement and implications of marine food security in the Western Indian Ocean: an impending crisis? *Food Security* **11**, 1395–1415. https://doi.org/10.1007/s12571-019-00971-6.

United Nations, Department of Economic and Social Affairs, Sustainable Development Goals. 2021 Available from: https://sdgs.un.org/goals/goal7.

Warner, K. J. & Jones, G. A. 2018 Energy and population in Sub-Saharan Africa: energy for four billion? *Environments* **5** (10), 107. https://doi.org/10.3390/environments5100107.

First received 3 October 2022; accepted in revised form 17 December 2022. Available online 26 December 2022